

## SIMULATION OF SUBGRIDBLOCK SCALE DNAPL POOL DISSOLUTION USING A DUAL DOMAIN APPROACH

Ronald W. Falta

Clemson University  
Brackett Hall, Room 340C  
Clemson, SC 29634-0919  
[faltar@clemson.edu](mailto:faltar@clemson.edu)

### **ABSTRACT**

A dual domain approach is used with an analytical solution for two-dimensional advection and dispersion to calculate the dispersive mass flux leaving a DNAPL pool inside a gridblock. The contaminated zone is first divided into two fractions: one which contains DNAPL pools, and one in which DNAPL is not present. With a dual permeability formulation, the two regions may have the same, or different flow properties, depending on the conceptual model for pool formation, and fluids can freely flow through both domains. The local dispersive flux of contaminant away from the pool is calculated using a well known analytical solution for steady-state advection and dispersion. This expression can be integrated analytically to give a first order mass transfer relationship for the total dissolution rate inside a gridblock as a function of the horizontal water velocity, the transverse dispersivity, the DNAPL solubility, and the dissolved concentration in the media not containing the DNAPL.

The method is demonstrated by simulation of a laboratory DNAPL pool dissolution experiment. Using the dual domain mass transfer model, the experimental dissolution rate data are matched in a T2VOC simulation using only 1 active dual domain gridblock. In contrast, a conventional modeling approach requires several thousand gridblocks to reproduce the experimentally observed dissolution rate. The method is then applied to a more complex situation involving several interacting DNAPL pools. The T2VOC dual domain simulation using only 1 or 2 dual domain gridblocks compares favorably with a semi-analytical solution for the steady state dissolution rate in this case. Numerical simulation of this problem with a conventional approach required at least 21,000 gridblocks to achieve a similar accuracy.

### **INTRODUCTION**

Chemical spills and releases involving DNAPLs in heterogeneous formations lead to the formation of thin layers or lenses of DNAPL in the subsurface known as DNAPL pools. These horizontal pools typically have a thickness of only a few cm or less, and they are characterized by a high NAPL phase saturation. As water (or gas above the water table)

flows through the contaminated zone, mass transfer from the DNAPL pool into the bulk fluid is limited by local transverse dispersion or diffusion away from the pool surface. It is possible to numerically simulate this dissolution process using a conventional multiphase flow approach, but a very fine grid is required, with discretization at the cm scale or less. This level of discretization is not practical for the simulation of three-dimensional field scale problems, in which there may be several DNAPL pools present.

Consider, for example, the DNAPL pool dissolution experiments conducted by Schuille (1988) shown in Figure 1. These experiments involved the emplacement of a thin layer of trichloroethylene (TCE) DNAPL in the bottom of the sand and water filled tank. Clean water was introduced at one end of the tank, and water contaminated with dissolved TCE was produced from the other end of the tank at groundwater pore velocities of 0.45 to 2.7 m/day.

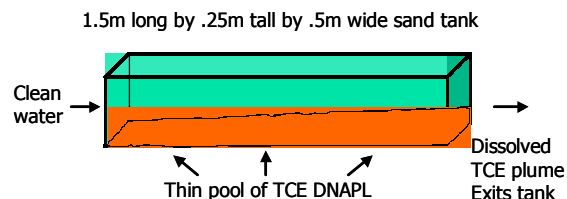


Figure 1. DNAPL pool dissolution experiment by Schuille (1988).

At pseudo-steady-state, the average concentration of dissolved TCE leaving the tank is much lower than TCE solubility due to the limited mass transfer of TCE from the DNAPL pool into the flowing water. TCE concentrations near the DNAPL pool, however are high, approaching the solubility of TCE.

The scale of Schuilles (1988) sand tank experiment is comparable to the scale of numerical discretization in a three-dimensional field scale multiphase flow numerical simulation. Thus, it is instructive to compare the rate of interphase mass transfer in a single gridblock assuming local chemical equilibrium (Local Equilibrium Assumption, LEA), to the rate of mass transfer observed in the experiments.

Assuming a DNAPL pool thickness of 1.5 cm, with a porosity of 0.34 and a NAPL saturation of 0.5, the initial mass of TCE in the 1.5m by 0.5m by 0.25m volume would be about 2.8 kg. For a LEA simulation, this TCE would be distributed throughout the gridblock at an average NAPL saturation of 0.03.

Figure 2 shows a T2VOC (Falta et al., 1995) simulation of the TCE dissolution assuming LEA in a single gridblock. The dissolved TCE concentration leaving the gridblock quickly reaches the TCE solubility of 1.1 g/l, and the DNAPL is completely dissolved in a short time. On the other hand, if the observed rate of TCE dissolution reported by Schwille (1988) from this experiment is used, the average TCE concentration in the effluent is only about 0.1 g/l, and the calculated time required for the DNAPL to be dissolved is approximately 10 times longer.

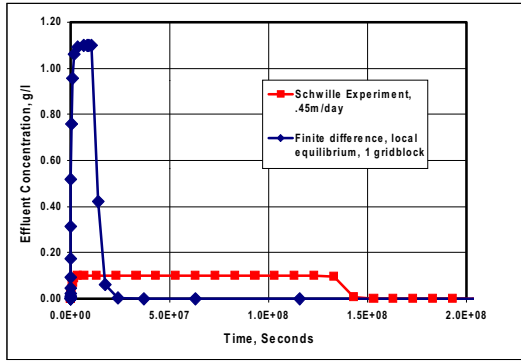


Figure 2. Prediction of DNAPL pool dissolution rate using a standard IFDM approach with one gridblock.

On the basis of this simulation result, it appears that the rate of DNAPL dissolution can easily be overestimated by a factor of 10 or more in field scale simulations if the DNAPL is in fact present as thin pools.

### DUAL DOMAIN FORMULATION

One approach to modeling the rate limited DNAPL pool dissolution inside a gridblock would be to use a first order heterogeneous interphase mass transfer reaction with a calibrated mass transfer rate. With this approach, a separate mass balance equation would be required for the chemical in the aqueous and NAPL phases. An alternative approach which preserves the LEA formulation used in the TOUGH codes, involves a dual domain approach to simulating the interphase mass transfer (see, for example, Falta, 2000).

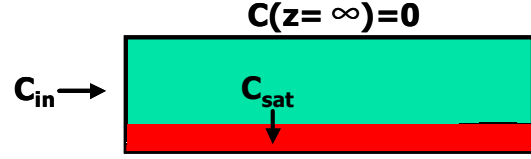


Figure 3. Boundary conditions for analytical pool dissolution solution by Hunt et al., (1988).

Considering a two-dimensional DNAPL pool dissolution geometry shown in Figure 3, and assuming pseudo-steady-state, Hunt et al. (1988) proposed the following differential equation and boundary conditions:

$$\begin{aligned} v \frac{\partial C}{\partial x} &= D_t \frac{\partial^2 C}{\partial z^2} & x=0, \quad C &= C_{in} \\ & & z=0, \quad C &= C_{sat} \\ D_t &= D_{eff} + v\alpha_t & z \rightarrow \infty, \quad C &\rightarrow 0 \end{aligned} \quad (1)$$

Where  $v$  is the water pore velocity,  $D_{eff}$  is the product of the tortuosity and the aqueous molecular diffusion coefficient,  $\alpha_t$  is the transverse dispersivity,  $C_{sat}$  is the NAPL solubility, and  $z$  is the vertical distance from the DNAPL pool. Equation (1) assumes that the dissolved concentration profile is steady in time, and it neglects dispersion in the direction of flow. The solution to equation (1) is (Hunt et al., 1988):

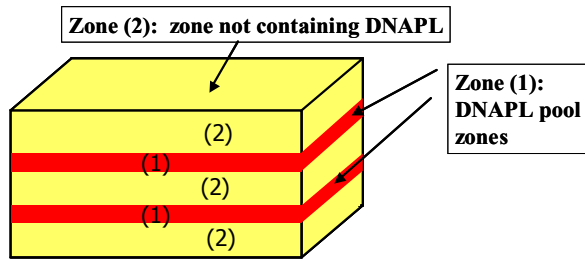
$$C = C_{in} + (C_{sat} - C_{in}) \operatorname{erfc} \left\{ \frac{z}{2\sqrt{D_t L_p / v}} \right\} \quad (2)$$

where  $L_p$  is the horizontal distance along the DNAPL pool. The pool surface-area-averaged dissolution mass flux,  $M_a$ , can be obtained by integrating the concentration with respect to  $z$  (Bird et al., 1960; Johnson and Pankow, 1992):

$$\begin{aligned} M_a &= \frac{v\phi}{L_p} \int_0^{\infty} C(L_p, z) dz \\ &= (C_{sat} - C_{in}) \phi \sqrt{4D_t v / (\pi L_p)} \end{aligned} \quad (3)$$

Johnson and Pankow (1992) showed that this expression provided a good match with the experimental data from the Schwille (1988) experiments. Equation (3) shows that the average dissolution mass flux from a DNAPL pool of length  $L_p$  can be approximated as a first order mass transfer reaction in terms of the inlet concentration and the DNAPL solubility.

In the present work, the dual permeability formulation in TOUGH (see, for example, Pruess et al., 1999) is modified to incorporate a transverse dispersive mass flux given by Equation (3). Figure 4 shows a conceptual diagram of a possible configuration for this dual domain geometry.



**Dual domain gridblock (actually two nodes are used, any geometry conceptually possible)**

Figure 4. Conceptualization of dual domain geometry for DNAPL pools. The DNAPL pool zone does not need to contain any NAPL, and the two zones can have any porous media properties.

Here, the DNAPL is shown to fully occupy zone (1), while the remainder of the porous medial is designated as zone (2). With the dual permeability formulation in TOUGH, zones (1) and (2) could be globally connected in a three-dimensional geometry (Pruess et al., 1999). With this configuration, water would be able to flow through both zones (1) and (2), so advective transport of the dissolved contaminant would be fully accounted for.

Normally, in a code such as T2VOC, the mass exchange between zone (1) and zone (2) would occur due to fluid potential and chemical concentration gradients between the two domains that would drive advection and diffusion. However, with the integral finite difference method (IFDM) used in TOUGH, mass flow terms between elements can be described by a conductance multiplied by a concentration difference. Therefore, the dispersive mass flow between zone (1) and zone (2) in Figure 4 could be simulated using the analytical solution for DNAPL pool dissolution, Equation (3):

$$\bar{M}_{12} = A_{12}(C_1 - C_2)\phi\sqrt{4D_t v_2 / (\pi L_p)} \quad (4)$$

where  $\bar{M}_{12}$  is the dispersive mass flow of chemical from the DNAPL pool (zone (1)) into the bulk porous media (zone (2)),  $C_1$  is the aqueous concentration of chemical in zone (1),  $C_2$  is the aqueous concentration of chemical in zone (2),  $A_{12}$  is the interfacial area between zone (1) and zone (2) in the gridblock, and  $v_2$  is the average horizontal water pore velocity in zone (2). This formulation is equivalent to a first order mass transfer reaction between zones (1) and (2).

Equation (4) was incorporated into the T2VOC code by modifying the MINC (see Pruess et al., 1999 and Falta, 2000) subroutines to allow for direct specification of the dual domain volumes, surface areas, and global connection parameters. The MULTI subroutine was modified to incorporate mass flows from Equation (4) when variable ISOT=4 in the CONNE data block. The parameters needed to for Equation (4),  $D_{eff}$ ,  $\alpha_t$ , and  $L_p$  are read through the SELEC data block.

It is important to fully couple the terms in Equation (4) with the Jacobian Matrix during each Newton Raphson iteration. The average horizontal water velocity in zone (2),  $v_2$ , is computed from the incremented water velocities in MULTI for directions ISOT=1,2. Similarly, the aqueous concentrations that appear in Equation (4) are calculated using the incremented aqueous mass fractions, and the transverse dispersion coefficient,  $D_t$ , uses the incremented  $v_2$ .

Several variations of this formulation are possible besides that shown in Figure 4. For example, the DNAPL pool zone (1) could be completely embedded inside zone (2) without any global connection to other gridblocks if the DNAPL pool length was much smaller than the gridblock length. In this case, the dispersive flux into zone (2) would still come from Equation (4), but there would be no advective transport through the pool zone into adjacent gridblocks. Similarly, for a small DNAPL pool, the global area connections for zone (1) could be reduced to be consistent with the small pool geometry, while still allowing for advective transport through the DNAPL pool. It is not necessary for zone (1) to contain any NAPL, and any porous media properties may be used in either zone.

## VALIDATION

### Simulation of Schwilles (1988) Laboratory Experiment

A series of T2VOC simulations were performed using one dual domain gridblock to represent the Schwille (1988) lab experiment geometry. The results of these simulations, for pore velocities ranging from 0.45 m/d to 2.7 m/d are shown in Figure 5.

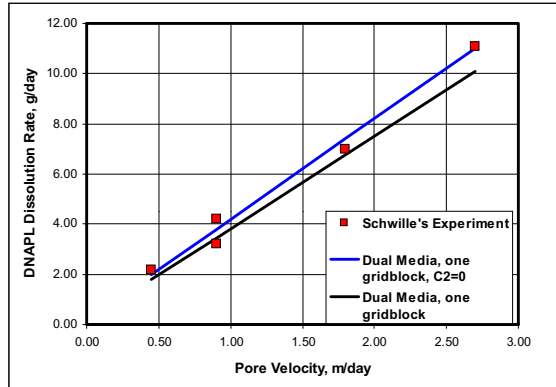


Figure 5. Simulation of Schwilles (1988) experiment using 1 dual domain IFDM gridblock.

The transverse dispersivity,  $\alpha_t$  was set at 0.25 mm. Two modeling approaches were used here, one where  $C_2$  was set to zero, as in the analytical solution, and one where  $C_2$  was the average concentration in zone (2). These two approaches produce a similar result, but the approach where  $C_2$  represents the concentration in zone (2) is preferable for larger scale applications because it prevents spurious dissolution mass flows from occurring when the background concentrations are high.

### Comparison With Sale and McWhorter (2001) Analytical Solution

Sale and McWhorter (2001) present a steady-state semi-analytical solution for DNAPL pool dissolution. Their solution assumes a uniform one-dimensional water flow field and it considers advection and transverse and longitudinal dispersion of the chemical in the aqueous phase, with kinetic interphase mass transfer inside the DNAPL pool regions. The DNAPL is assumed to be immobile, and water flows freely through the DNAPL pool without any relative permeability effects. Based on their steady-state results, Sale and McWhorter (2001) conclude that "removal of the vast majority of the DNAPL will likely be necessary to achieve significant near-term improvements in water quality".

As an example of the application of their model, Sale and McWhorter (2001) present a two-dimensional case with multiple DNAPL source zones as shown in Figure 6.

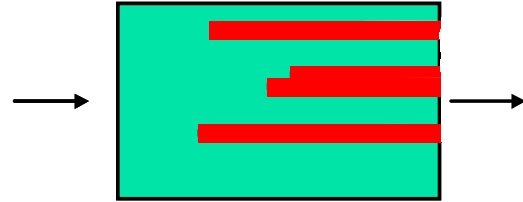


Figure 6. Two-dimensional DNAPL pool geometry considered by Sale and McWhorter (2001).

This problem has dimensions of about 6m by 3.5m by 1m thick, with five 1m long DNAPL pools. Each DNAPL pool has a vertical thickness of 0.1m. The water pore velocity was 0.1 m/d, the transverse dispersivity ( $\alpha_t$ ) was 1mm, the longitudinal dispersivity was 0.1m, and molecular diffusion was neglected.

A conventional T2VOC simulation of this case was run to illustrate the difficulty of capturing the local scale mass transfer that occurs near DNAPL pools. The Sale and McWhorter example above was presented in terms of dimensionless mass transfer rates, so a porosity of 0.35, and a DNAPL solubility of 0.11 g/l were selected. The DNAPL saturation inside the pool zones is not a parameter in the Sale and McWhorter model, so a value of 0.05 was assumed for the T2VOC simulation. The relative permeability of water was set to one, and the relative permeability of NAPL was set to zero.

The T2VOC code does not consider the hydrodynamic dispersion tensor, but the modified version used here includes aqueous phase molecular diffusion. Because the water flow field in this example is uniform and constant, it is possible to simulate isotropic dispersion by setting the aqueous diffusion coefficient in the modified T2VOC code equal to the transverse dispersion coefficient ( $\alpha_t v$ ) with a tortuosity of 1. This provides an accurate approximation of the transverse dispersion for this case, but it underestimates the longitudinal dispersion. Numerical dispersion in the direction of flow due to upstream weighting of the concentration is often a concern, but in this problem, the sharp concentration profiles associated with the leading edges of the dissolved plumes leave the problem domain after a short time.

A fine (conventional) numerical grid was used with a vertical grid spacing of 1 cm, and a horizontal grid spacing of 10 cm. Therefore, each DNAPL pool was modeled with 10 layers and 10 rows of gridblocks, and a total of 21,000 active gridblocks were used. Figure 7 shows the initial aqueous chemical concentrations in the simulation domain. Within the DNAPL zones, the dissolved concentration is at the solubility of 0.11 g/l.

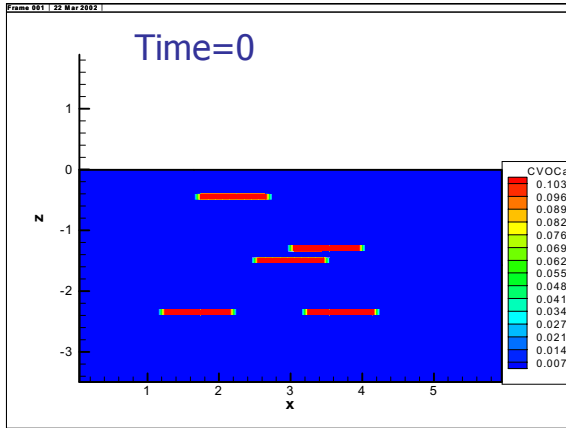


Figure 7. Initial dissolved chemical concentrations for transient T2VOC simulation with 21,000 gridblocks. The DNAPL pools contain a DNAPL saturation of 0.05 initially.

Figures 8, 9, and 10 show the simulated dissolved chemical profiles after 181 days, 11.2 years, and 23.8 years, respectively.

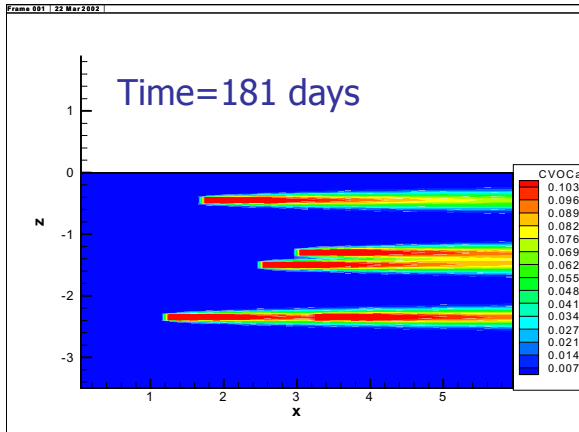


Figure 8. Simulated dissolved chemical concentrations after 181 days.

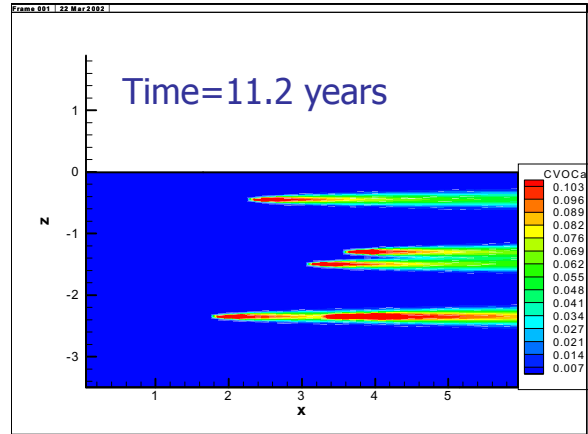


Figure 9. Simulated dissolved chemical concentrations after 11.2 years.

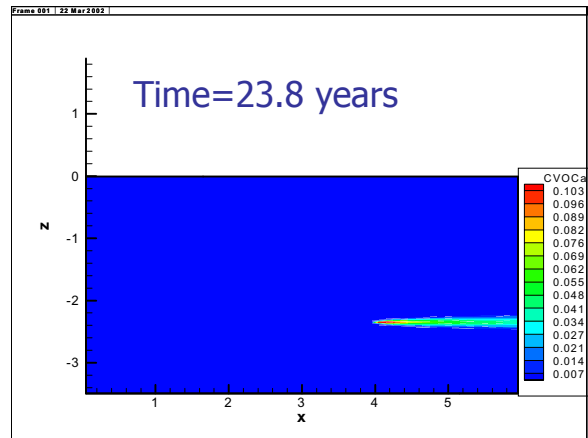


Figure 10. Simulated dissolved Chemical concentrations after 23.8 years.

As the DNAPL pools dissolve, it is apparent that the effluent concentration also decreases as the pools become thinner and shorter. After approximately 17 years, the upper pools have dissolved away, leaving only one lower pool. This DNAPL zone was located downstream of a dissolving pool, so the dissolution mass transfer from this pool was relatively slow until the upstream DNAPL was removed. The 21,000 gridblock T2VOC simulation took 3.25 hours to run on an 800 MHz PC.

Figure 11 shows the time-dependent DNAPL dissolution rate during the T2VOC simulation. The maximum dissolution rate (measured leaving the simulation domain) occurs essentially at time zero, and the magnitude is close to that predicted by the Sale and McWhorter (2001) steady state solution. It is possible that an even finer grid, or the inclusion of longitudinal dispersion in the T2VOC simulation would produce a better match with the semi-analytical solution. An earlier simulation with only 2100



gridblocks resulted in a poor match with the steady state solution.

As the DNAPL mass is removed from the system, the rate of dissolution steadily drops due to the reduced DNAPL contact with the flowing water. A distinct change in slope occurs at about 17 years, when the upper pools disappear, leaving only the second lower pool. After about 26 years, all of the DNAPL has been removed from the system.

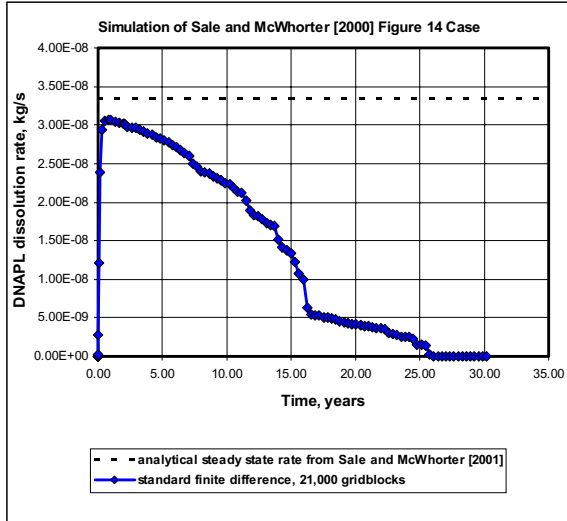


Figure 11. Comparison of numerically simulated transient DNAPL dissolution rate with steady-state solution of Sale and McWhorter (2001).

While the time scale for DNAPL mass removal in this simulation depends on both the initial NAPL saturation on the chemical solubility, it is very clear that as the DNAPL mass is removed, the dissolution rate decreases. Therefore, impacts to a groundwater system would be expected to similarly decrease with partial DNAPL mass removal. This observation appears to contradict the conclusion of Sale and McWhorter (2001) about the effect of DNAPL removal on the resulting groundwater quality.

To illustrate the new dual domain mass transfer approach, the Sale and McWhorter example was modeled using T2VOC with a single active dual domain gridblock. The zone (1) and zone (2) volumes were calculated using the conceptual model shown in Figure 4 to allow for advective flow through, and out of, zone (1). Thus, the volume of zone (1) in this simulation was  $4 \times 6\text{m} \times 0.1\text{m} \times 1\text{m} = 2.4\text{m}^3$ , and the volume of zone (2) was  $21\text{m}^3 - 2.4\text{m}^3 = 18.6\text{m}^3$ . The global connection area of zone (1) to the inlet and outlet elements was  $4 \times 0.1\text{m} \times 1\text{m} = 0.4\text{m}^2$ , while the global connection area of zone (2) to the inlet and outlet elements was  $3.5\text{m}^2 - 0.4\text{m}^2 = 3.1\text{m}^2$ .

The zone (1)/zone (2) interfacial area was calculated as  $2 \times 5 \times 1\text{m} \times 1\text{m} = 10\text{m}^2$ , and the pool length was specified as 1m. Figure 12 shows the results of this simulation, compared to the analytical solution and the conventional fine grid simulation. The single dual domain gridblock very nearly reproduces the dissolution rate predicted by the steady-state semi-analytical solution. It also gives a result that is reasonably close to the conventional fine grid simulation, although the time for complete DNAPL removal is underestimated by about 10 years. The dual domain simulation here took 0.14 seconds on the same 800 MHz PC that took 3.25 hours to run the conventional fine grid simulation.

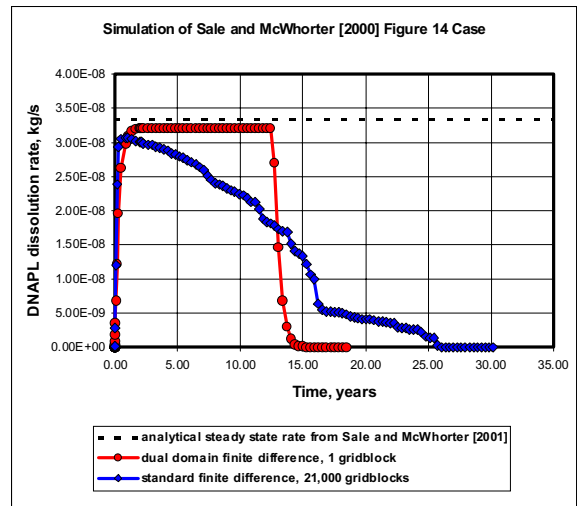


Figure 12. Comparison of IFDM simulation using 1 dual domain gridblock with result using 21,000 gridblocks.

Figure 13 shows the vertical profile of peak dissolved chemical concentration leaving the right edge of the flow domain from the conventional simulations, compared to the zone (1) and zone (2) concentrations calculated during the dual domain simulation. Although the figure assigns a vertical location for the zone (1) and zone (2) concentrations, this is only for purposes of illustration, as such information is not recorded or used in the simulation. The peak dissolved concentration in zone (1) is equal to the chemical solubility of 0.11 g/l, while the dissolved concentration in the bulk zone (2) is about 0.01 g/l. This figure illustrates the fact that the dual permeability formulation is capable of approximating the large contrasts in chemical concentrations that can occur over the scale of a gridblock.

The dual domain model can be refined somewhat for this case by using two gridblocks, one for the upper half of the problem, and one for the lower half of the problem. Splitting the problem this way allows for the upper 3 pools to be contained in one dual domain

gridblock, with the lower 2 pools in a second dual domain gridblock. Because the lower 2 pools are in series, this simulation configuration is better able to reproduce the longer life of the DNAPL in the downstream lower pool. The model parameters for this simulation were calculated in the same way as in the previous case, but zone (1) in the lower gridblock contains twice the DNAPL saturation because two pools fall into one 0.1m thick zone. The pool length in this block was set to 2m instead of 1m.

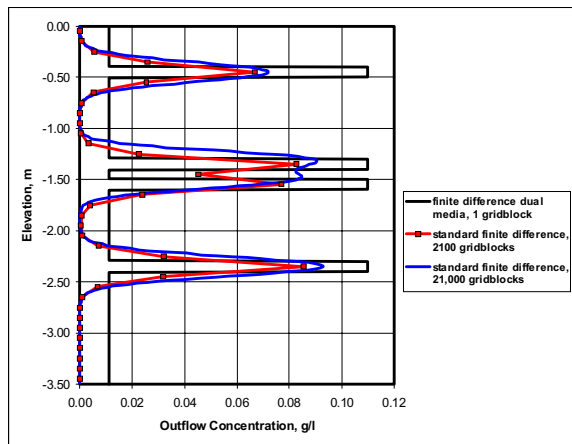


Figure 13. Dissolved chemical concentration profiles at the outlet for numerical simulations with 21,000, and 2,100 conventional gridblocks, and with 1 dual domain gridblock.

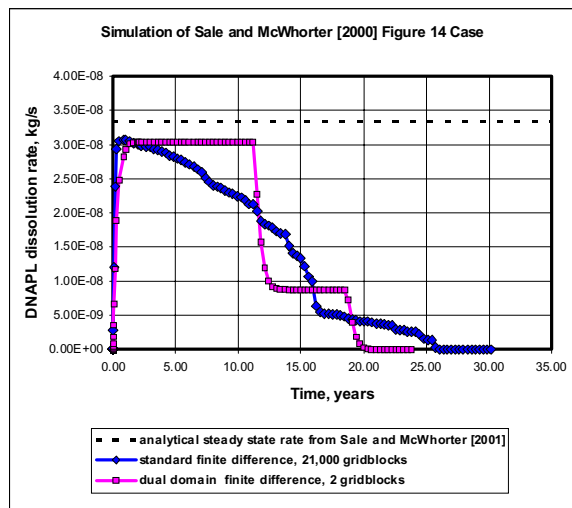


Figure 14 Comparison of IFDM simulation using 2 dual domain gridblocks with result using 21,000 gridblocks.

Figure 14 shows the results of this simulation, compared to the fine grid conventional simulation. As expected, the two element dual domain model captures the transient effects better than the single

element model, and the predicted time for complete DNAPL removal is only about 5 years different from the fine grid simulation.

## DISCUSSION

It appears that this relatively straightforward approach for modeling DNAPL pool dissolution could be useful for field scale simulations of chemical transport and remediation. Although not mentioned here, extensions to rate limited NAPL evaporation during soil vapor extraction in layered systems are obvious.

There are, however important theoretical and practical issues that need to be addressed to make this technique practical. Considering the fact that the real geometry of DNAPL pools in the field is essentially unknown, direct measurement of the mass transfer parameters needed in this model is not possible. The mass transfer model only accounts for vertical dispersion, but lateral dispersion could be significant in some cases.

The effects of vertical flows through DNAPL pools could be very significant, and it is not clear what the best way of representing this type of mass transfer would be. The current implementation assumes that some fraction (user input) of the vertical flow in zone (2) flows through zone (1), and contributes to the overall dissolution mass flow between the domains.

Finally, it is not known whether or not it will be possible to realistically model a DNAPL spill with this approach. It does seem possible though, that the properties of the two domains could be used to approximate the subgridblock scale heterogeneity that causes the small DNAPL pools to begin with.

## ACKNOWLEDGMENT

This work was supported in part by an EPA Cooperative Agreement, Assistance ID No. R-83082901-0, with funding provided by the Strategic Environmental Research and Development Program (SERDP). It has not been subjected to Agency review and, therefore, does not necessarily reflect the views of the Agency and no official endorsement should be inferred.

## REFERENCES

Bird, R. B., W. E. Stewart, and E. N. Lightfoot, *Transport Phenomena*, John Wiley, New York, 1960.

Falta, R.W. Numerical modeling of kinetic inter-phase mass transfer during air sparging using a dual-media approach, *Water Resources Research*, Vol. 36, No. 12, 2000.

Falta, R.W., K. Pruess, S. Finsterle, and A. Battistelli, *T2VOC User's Guide*, Lawrence Berkeley Laboratory Report LBL-36400, March, 1995.

Hunt, J. R., N. Sitar, and K.S. Udell, Nonaqueous phase liquid transport and cleanup, 1, Analysis of mechanisms, *Water Resources Research*, Vol 24, No. 8, 1247-1258, 1988.

Johnson, R. L., and J. F. Pankow, Dissolution of dense chlorinated solvents into groundwater. 2. Source functions for pools of solvent, *Environ. Sci. Technol.*, Vol. 26, No. 5, 896-901, 1992.

Pruess, K., C. Oldenburg, and G. Moridis, *TOUGH2 User's Guide, Version 2.0*, Report LBNL-43134, Lawrence Berkeley National Laboratory, Berkeley, Calif., 1999.

Sale, T. C., and D. B. McWhorter, Steady state mass transfer from single-component dense nonaqueous phase liquids in uniform flow fields, *Water Resources Research*, Vol. 37, No. 2, 393-404, 2001.

Schwille, F., *Dense Chlorinated Solvents in Porous and Fractured Media – Model Experiments*, Translated by J. F. Pankow, Lewis Publishers, Boca Raton, FL, 1988.